

# Evaluation of dental and basal arch forms using cone-beam CT and 3D virtual models of normal occlusion

Mohamed Bayome,<sup>\*</sup> Jae Hyun Park,<sup>†</sup> Seong Ho Han,<sup>‡</sup> Seung-Hak Baek,<sup>‡</sup> Glenn T. Sameshima<sup>‡</sup> and Yoon-Ah Kook<sup>§</sup>

The Catholic University of Korea, Seoul, Korea,<sup>\*</sup> Arizona School of Dentistry & Oral Health, A. T. Still University, Mesa, Arizona, USA and Graduate School of Dentistry, Kyung Hee University, Seoul, Korea,<sup>†</sup> Department of Orthodontics, St. Vincent Hospital, The Catholic University of Korea, Seoul, Korea,<sup>‡</sup> School of Dentistry, Dental Research Institute, Seoul National University, Seoul, Korea,<sup>‡</sup> Department of Orthodontics, School of Dentistry, University of Southern California, Los Angeles, California, USA<sup>‡</sup> and Department of Orthodontics, Seoul St. Mary's Hospital, The Catholic University of Korea, Seoul, Korea<sup>§</sup>

**Objectives:** To evaluate the relationship between the mandibular dental and basal arches using CBCT, and to assess the correlation between basal arch dimensions derived from CBCT and 3-dimensional (3D) virtual models in a cohort sample exhibiting normal occlusions.

**Methods:** The facial axis (FA) and root centre (RC) points of mandibular teeth were identified on 32 CBCT images. FA and WALA points were digitised on 3D models of 28 mandibular casts from the same sample. The relationships between dental and basal arch dimensions, and between the two basal depth dimensions derived from RC and WALA points were statistically assessed by Pearson's correlation.

**Results:** Strong correlations were found between dental and basal intercanine and intermolar arch widths. Also, the basal intercanine width showed a moderate correlation with dental intermolar width and depth. The basal intercanine and intermolar widths measured on 3D models showed moderate correlations with those measurements on CBCT, whereas the basal canine and molar depths showed no correlations.

**Conclusions:** The dental and basal anterior and posterior arch widths were strongly correlated in normal occlusion. No correlations were found between the arch depths measured from WALA points and RC points. Hence, RC points may represent more useable landmarks compared to WALA points in the evaluation of basal arch forms. It is recommended that the relationship between the dental and basal arches is evaluated during treatment planning in order to improve arch co-ordination.

(Aust Orthod J 2013; 29: 43-51)

Received for publication: May 2012

Accepted: February 2013

Mohamed Bayome: mohamed@catholic.ac.kr; Jae Hyun Park: jpark@atsu.edu; Seong Ho Han: seonghh@hotmail.com; Seung-Hak Baek: drwhite@unitel.co.kr; Glenn T. Sameshima: sameshim@usc.edu; Yoon-Ah Kook: kook190036@yahoo.com

## Introduction

An understanding of the relationship between dental and basal arch forms is of diagnostic and therapeutic importance because expansion of the dental arch has clinical limitations. There is an increased risk of relapse and periodontal complications if teeth are moved farther than their apical base limits.<sup>1-5</sup> The shape of

the basal arch form has seldom been analysed, whereas dental arch form has been frequently assessed.<sup>6-16</sup> Most studies have examined the dental arch using 2-dimensional (2D) methods,<sup>10-22</sup> but digitised incisal edges and cusp tips or contact points in past studies were imprecise representations of clinical arch forms.

Contemporary research has evaluated arch dimensions from facial axis (FA) points measured in three dimensions (3D).<sup>23,24</sup> Because digitising FA points in a 2D manner is not reliable, an analysis using a 3D method appears clinically relevant, particularly when the use of preformed superelastic archwires is commonly considered.

The relationship between dental and basal arch forms has been evaluated using the WALA (an acronym for Will Andrews and Larry Andrews, who jointly proposed a band of soft tissue immediately superior to the mucogingival junction [MJG] in the mandible) ridge that connects the most convex points on the MGJ.<sup>25-28</sup> A highly significant correlation between dental and basal widths in the canine and molar areas was reported. Kim et al.<sup>29</sup> demonstrated that different dental arches showed only minimal differences in their skeletal arch dimensions, and presented moderate correlations between basal and dental intercanine widths. Therefore, it was suggested that basal arch form might not be a principal factor in determining dental arch form. Furthermore, uncertainty existed because the definition of the basal arch by WALA points could be affected by soft tissue changes and the variable angulations of tooth roots may be difficult to determine.

With the advent of cone-beam computed tomography (CBCT), new landmarks have been defined, particularly the centre of tooth resistance (COR), on CBCT images. Changes in the basal arch under orthodontic forces might be expressed more accurately using this landmark, rather than using the WALA points on a virtual model. Recently, CBCT was used by Tai et al.<sup>30</sup> to evaluate mandibular basal bone change after the placement and treatment using a Schwarz appliance. However, there remains no description of the relationship between the COR of the mandibular teeth and FA points on a CBCT image. In addition, there has been no comparison of dental and basal arch dimensions measured on CBCT images and 3D digital models. Information in this area may help the clinician identify the most appropriate location of tooth roots in relation to arch form.

The aims of this study were to evaluate the relationship between the mandibular dental and basal arches using CBCT, and also to assess the relationship between the basal arch dimensions measured on CBCT and those derived from 3D virtual models in a sample representing normal occlusions.

## Material and methods

Thirty-two young adults (19 males, 13 females; mean age, 24.3 years) with normal occlusions were recruited from the College of Dentistry, Wonkwang University, Iksan, Korea and the Nursing School of the Catholic University of Korea in Seoul. Approval for this study was obtained from the institutional review board of the Catholic University of Korea, Catholic clinical research coordinating centre (IRB No. KC11EASE0182), and informed consent was provided according to the Declaration of Helsinki.

The inclusion criteria were a full permanent dentition (excluding third molars) in a Class I molar and canine relationship, arch length discrepancies of less than 3 mm, a normal curve of Spee of less than 2 mm, an absence of dental rotations, a normal overbite and overjet, coincidental facial and dental midlines, an absence of extensive restorations and no previous orthodontic treatment.

CBCT images were acquired with an Alphard 3030 (Asahi Roentgen Ind. Co., Ltd., Kyoto, Japan) (80 KV, 5 mA and a scanning time of 17 seconds). A 200 × 179 mm field and a voxel size of 0.39 mm were used. The axial images were exported in digital imaging and communication in medicine (DICOM) format. Invivo 5.1 (Anatomage, San Jose, CA, USA) was used to reconstruct the axial images, view, digitise and measure the CBCT scans.

An initial re-orientation of head position of each scan was performed. The contact point between the mandibular central incisors (MCI) was selected as the origin of the X, Y and Z coordinates. The image was subsequently rotated so that the horizontal reference plane (X) coincided with an occlusal plane connecting the mesiobuccal cusp tip of the right and left mandibular first molars and the MCI origin. The midsagittal plane (Y) was defined by a line passing through MCI, and parallel to a line connecting the anterior and posterior nasal spines. The vertical plane (Z) was defined as the perpendicular to both X and Y.

To assist in the evaluation of dental arch dimensions on the CBCT scan, facial axis (FA) points<sup>31</sup> of the mandibular teeth from right first molar to left first molar were digitised on the volume rendering view using the bone settings of Invivo 5.1 software (Figure 1a). Basal arch dimensions on the CBCT scan were evaluated by the digitisation of the root centre (RC) on a transverse section parallel to the occlusal plane

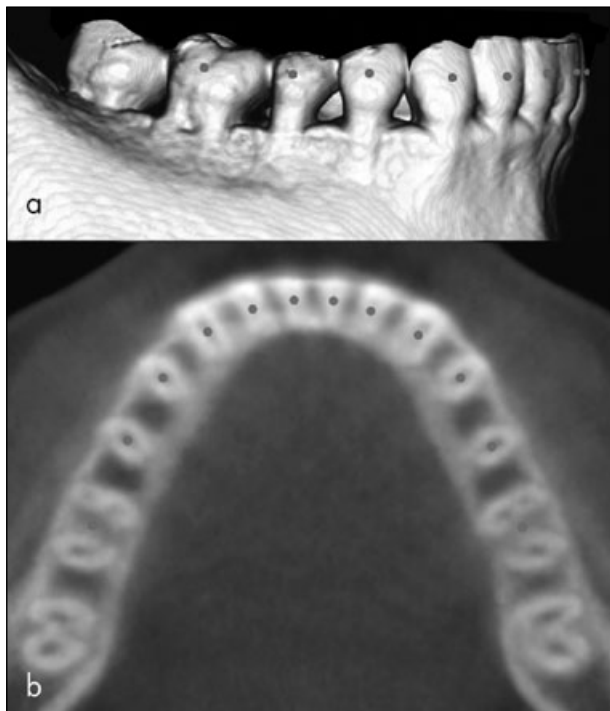


Figure 1. Digitised rendered view of a CBCT scan: (a) Facial axis (FA) points; (b) Root centre (RC) points.

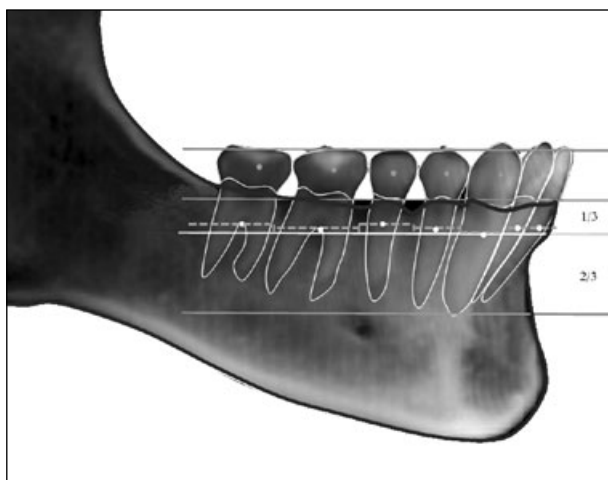


Figure 2. Schematic drawing for basal arch identification. Dots; Facial axis (FA) points, Dotted/dashed line; interrupted arch connecting each tooth's centre of resistance, White line; continuous arch parallel to the occlusal plane at the level of the coronal 1/3 of canine roots.

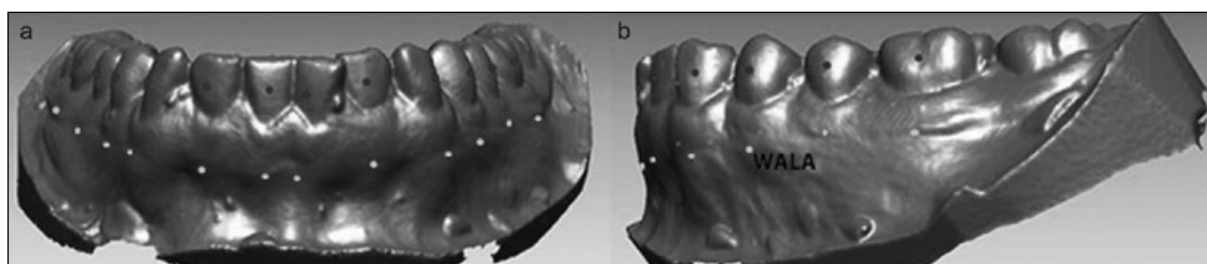


Figure 3. The facial axis (FA) points (black) and WALA points (white) digitised on a 3D model: (a) Frontal view; (b) Lateral view.

at the level of the coronal 1/3 of the canine roots (Figures 1b and 2). This transverse section was chosen because of its proximity to the WALA points<sup>25</sup> which are located at the most convex point on the MGJ directly below the intersection of FA perpendicular to the occlusal plane. Four linear and two ratio variables were calculated for each dental and basal arch form (Table I).

Due to unavailability, only 28 mandibular casts were obtained from the identified sample to evaluate the dental and basal arch dimensions on the digital models. The casts were scanned with an Orapix KOD-300 3D laser scanner (Orapix Co., Ltd, Seoul, Korea) at a 20-micrometre-unit resolution. Two reference points, FA point and WALA point, were digitised for each tooth from the right to the left mandibular first molar on each virtual model using Rapidform 2006 software (INUS technology, Inc., Seoul, Korea) and used to represent dental and basal arch forms, respectively (Figure 3).

Plane X was the horizontal direction, plane Y the antero-posterior (midsagittal) direction, and plane Z was the perpendicular to both. The contact point between the MCIs was set as the origin, and the Z-values were nullified for easier geometrical and mathematical processing. The same arch form variables were calculated for each case (Table I).

All digitisation was performed by one investigator (MB) who had experience in the 3D technology. To assess the reliability of the digitising process, ten CBCT scans and ten 3D models were redigitised 2 weeks later.

### Statistical analysis

Statistical evaluation was performed using SPSS version 16 (SPSS Inc., Chicago, IL, USA). The intra-class correlation coefficient (ICC) between the duplicate measurements showed high reliability (ICC

**Table I.** Definitions of mandibular arch form variables.

	Definition
FA points	The middle of the axis of the facial surface of each tooth on the CBCT images and the 3D virtual casts
RC points	The centre of the root on a transverse section parallel to the occlusal plane at the level of the coronal 1/3 of the canine roots on the CBCT images
WALA points	The most convex point on the MGJ directly below FA perpendicular to the occlusal plane on the 3D virtual casts
<i>Dental arch</i>	
Dental intercanine width	The distance between the FA points of the right and left canines
Dental intermolar width	The distance between the FA points of the right and left first molars
Dental intercanine depth	The shortest distance from a line connecting the FA points of the right and left canines to the origin
Dental intermolar depth	The shortest distance from a line connecting the FA points of the right and left first molars to the origin
Dental intercanine width/depth ratio	Ratio between dental intercanine width and depth
Dental intermolar width/depth ratio	Ratio between dental intermolar width and depth
<i>Basal arch</i>	
Basal intercanine width	The distance between the RC points of the right and left canines on CBCT, or their WALA points on 3D model
Basal intermolar width	The distance between the RC points of the right and left first molars on CBCT, or their WALA points on 3D model
Basal intercanine depth	The shortest distance from a line connecting the RC or WALA points of the right and left canines to the midpoint between the RC or WALA points of the central incisors on CBCT or 3D models, respectively
Basal intermolar depth	The shortest distance from a line connecting the RC or WALA points of the right and left first molars to the midpoint between the RC or WALA points of central incisors on CBCT or 3D models, respectively
Basal intercanine width/depth ratio	Ratio between basal intercanine width and depth
Basal intermolar width/depth ratio	Ratio between basal intermolar width and depth

FA = Facial axis; RC = root centre; WALA = acronym for Will Andrews and Larry Andrews, who jointly proposed a band of soft tissue immediately superior to the mucogingival junction in the mandible

> 0.8). Normal distribution of the parameters was assessed by the Kolmogorov-Smirnov test. The dental arch dimensions measured on the CBCT image and 3D models were compared by a paired *t*-test. The relationship between the 2 representations of the basal arch form, RC and WALA, was assessed using Pearson's correlation coefficient. Pearson's correlation coefficient was further employed to examine the correlations between dental and basal arch dimensions measured on the CBCT images. An analysis of variance (ANOVA) was performed to compare the distances between corresponding FA and RC points associated with the different areas of the arch forms.

## Results

The dental and basal arch dimensions measured on CBCT and 3D digital models are presented in Table II. There were no significant differences between the dental arch dimensions measured on the CBCT scans and those measured on the 3D models. The measurement of the basal arch dimensions using RC and WALA points revealed a statistically significant moderate correlation in the intercanine ( $r = 0.58$ ,  $p = 0.007$ ) and intermolar widths ( $r = 0.64$ ,  $p = 0.002$ ); however, no correlation was found in arch depths (Figure 4 and Table III).

**Table II.** Dental and basal arch dimensions measured on CBCT and 3D digital model.

	FA on CBCT N = 32		FA on 3D model (N = 28)		p value	RC on CBCT (N = 32)		WALA on 3D model (N = 28)	
	Mean	SD	Mean	SD		Mean	SD	Mean	SD
Intercanine width (mm)	29.55	1.55	29.70	1.60	NS	23.85	1.44	31.05	2.52
Intermolar width (mm)	54.17	3.06	53.47	3.05	NS	49.95	3.35	55.78	3.49
Intercanine depth (mm)	4.54	0.91	4.33	0.77	NS	3.88	0.68	4.84	1.27
Intermolar depth (mm)	26.52	1.71	25.94	1.49	NS	26.35	1.74	25.42	5.20
Intercanine width/depth	6.78	1.46	7.05	1.30	NS	6.31	1.11	6.65	1.29
Intermolar width/depth	2.05	0.14	2.07	0.15	NS	1.90	0.13	2.36	0.91

Paired *t* test; NS = not significant

FA = Facial axis; RC = Root centre

**Table III.** Correlations among arch dimensions measured from RC points and WALA points (N = 28).

RC	WALA		ICW		ICD		IMW		CWD		IMD		MWD	
	r	p	r	p	r	p	r	p	r	p	r	p	r	p
Intercanine width (ICW)	0.58	0.007	0.24	NS	0.30	NS	-0.15	NS	-0.08	NS	0.23	NS		
Intercanine depth (ICD)	0.20	NS	0.35	NS	-0.15	NS	-0.08	NS	-0.31	NS	0.16	NS		
Intermolar width (IMW)	0.35	NS	-0.23	NS	0.64	0.002	0.06	NS	0.27	NS	-0.15	NS		
Intermolar depth (IMD)	0.38	NS	0.06	NS	0.25	NS	0.00	NS	-0.01	NS	0.02	NS		
Intercanine width/depth (CWD)	0.00	NS	-0.26	NS	0.28	NS	0.06	NS	0.27	NS	-0.10	NS		
Intermolar width/depth (MWD)	-0.01	NS	-0.28	NS	0.40	NS	0.05	NS	0.27	NS	-0.18	NS		

r = Pearson correlation coefficient; NS = not significant

RC = Root centre

**Table IV.** The horizontal distance between the FA and RC points (FA-RC distance) (Unit: mm).

	Central incisor	Lateral incisor	Canine	1st premolar	2nd premolar	1st molar	p value
Mean	5.55 a	5.39 a	5.48 a	4.78 b	4.41 b	5.92 b	< 0.001
SD	1.34	1.25	0.98	0.92	0.81	1.16	

ANOVA and Tukey's post-hoc test

FA = Facial axis; RC = Root centre

a = no significant difference

b = no significant difference, however there was significant difference between a and b

**Table V.** Correlations between dental and basal arch dimensions on CBCT (N = 32).

Basal	ICW		IMW		ICD		IMD		CWD		MWD		
	Dental	r	P	r	P	r	P	r	P	r	P	r	P
ICW	0.69	<0.001	0.31	NS	0.34	NS	0.57	0.001	-0.07	NS	-0.27	NS	
IMW	0.58	<0.001	0.78	<0.001	0.14	NS	0.51	0.003	0.09	NS	0.26	NS	
ICD	0.26	NS	0.17	NS	0.20	NS	0.45	0.009	-0.08	NS	-0.30	NS	
IMD	0.49	0.005	0.21	NS	0.33	NS	0.56	0.001	-0.12	NS	-0.36	0.043	
CWD	-0.15	NS	-0.22	NS	-0.06	NS	-0.36	0.041	-0.03	NS	0.15	NS	
MWD	-0.13	NS	0.28	NS	-0.25	NS	-0.27	NS	0.19	NS	0.56	0.001	

r = Pearson correlation coefficient; NS = not significant

ICW = Intercanine width; IMW = intermolar width; ICD = intercanine depth; IMD = intermolar depth; CWD = intercanine width/depth;

MWD = intermolar width/depth

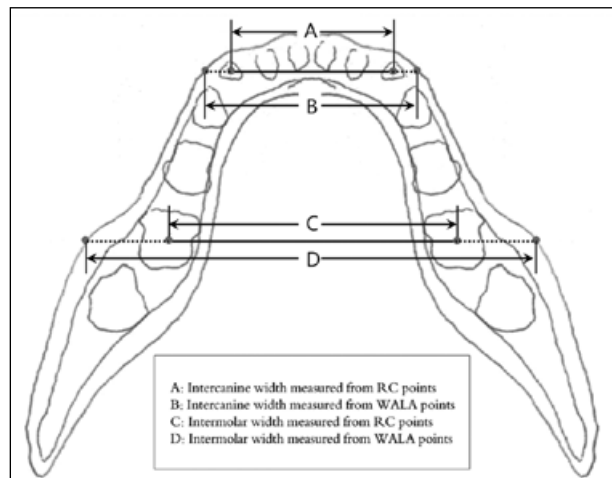


**Figure 4.** Schematic drawing of measured arch dimensions. A, intercanine width measured from RC points; B, intercanine width measured from WALA points; C, intermolar width measured from RC points; D, intermolar width measured from WALA points.

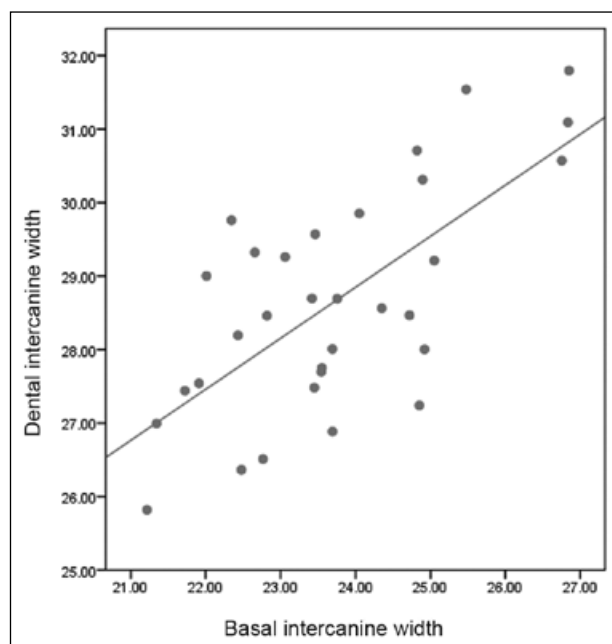


**Figure 5.** Scatterplot showing the correlation between the dental and basal intercanine widths of the normal occlusion samples. The correlation coefficient ( $r$ ) is 0.69, and the  $p$  value is  $< 0.001$ .

The mean horizontal distances between corresponding FA and RC points on the CBCT images are presented in Table IV. There was no significant difference in the mean FA-RC distance at the first and second premolars. Similar horizontal measurements of distances between corresponding FA and RC points at the incisors, canines, and first molars also showed no significant differences. However, the distances

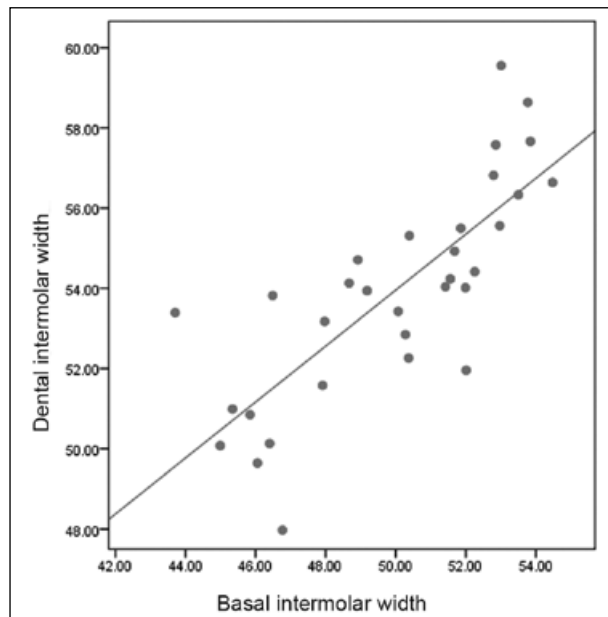


**Figure 6.** Scatterplot showing the correlation between the dental and basal intermolar widths of the normal occlusion samples. The correlation coefficient ( $r$ ) is 0.78, and the  $p$  value is  $< 0.001$ .

measured at the premolars were significantly smaller ( $p < 0.001$ ) than those measured at the other teeth.

A strong CBCT-evaluated correlation was found between dental and basal intermolar widths ( $r = 0.78$ ;  $p < 0.001$ ), as well as between dental and basal intercanine widths ( $r = 0.70$ ;  $p < 0.001$ ) (Figures 5 and 6). Moreover, the basal intercanine width showed moderate correlation with the dental intermolar width and depth ( $r = 0.58$  and  $0.49$ ,  $p < 0.001$  and  $p < 0.005$ , respectively).

In addition, moderate correlations were found between the basal intermolar depth and each of the dental intercanine widths and depths, as well as the intermolar width and depth. The basal intermolar depth demonstrated a weak reverse correlation with the dental intercanine width/depth ratio. Furthermore, the basal intermolar width/depth ratio showed a moderate correlation with its dental counterpart and a weak reverse correlation with the dental intermolar depth (Table V).

## Discussion

To establish a dental arch form in a harmonious relationship with the underlying basal bone is one of the important goals of orthodontic treatment. Therefore, the present study has attempted to assess

the relationship between dental and basal arch dimensions through CBCT scans. This evaluation of the dento-skeletal relationship of arch forms in subjects possessing normal occlusions may eventually help clinicians recognise instability between dental and skeletal arches and establish a compatible relationship as an orthodontic treatment aim.

The determination and analysis of this relationship requires an exact definition of the basal arch. The current definition of basal bone or basal arch is ambiguous and controversial, particularly in the determination of its vertical position in the alveolar process. Lundström<sup>2</sup> defined basal bone as the horizontal plane in which the apices of the tooth roots were located. However, Howes<sup>7</sup> described it as the apical third of the alveolus and its supporting bone as it contained the most constricted area of the alveolus and was generally about 8 mm apical to the gingival margin.

Later, Andrews and Andrews<sup>25</sup> suggested a modified clinical representation of the apical base proposed by Lundström,<sup>2</sup> as the band of keratinized soft tissue directly adjacent to the MGJ which was called the WALA ridge. Alternatively, an evaluation of basal bone by Sergl et al.,<sup>8</sup> recorded the most concave soft tissue contour in relation to the tooth apices on dental casts. In the present study, basal arch was defined as the horizontal band that passes through the centres of the roots at the vertical level of the junction between the gingival and middle third of the canines.

Conventionally, basal arch dimensions on dental casts have been measured from various landmarks, such as the apical one-third of the alveolar bone approximately 9 mm below the gingival margin or at the innermost points of the buccal folds.<sup>6,8,9,32</sup> Additional studies have compared the relationship between dental and basal arch forms in different malocclusion groups using WALA points.<sup>26,28</sup> Interestingly, most of the studies which have evaluated basal arch form placed landmarks on alveolar bone rather than basal bone.<sup>7,8,26-29</sup> Therefore, the term 'basal arch' used in previous and current research represents a misnomer. However, this defined basal arch, or more accurately 'alveolar arch', may be more important for clinical application than anatomical basal bone, since the alveolar process is the investing structure of the teeth.

A previous study reported a moderate correlation between intercanine dental and basal widths, and a strong correlation between the intermolar widths using

FA and WALA landmarks on 3D virtual models of normal occlusions.<sup>29</sup> The present results also indicated that the dental and basal arch widths measured on CBCT images were strongly correlated. The dental and basal intermolar depths demonstrated moderate correlation, but a similar positive relationship was not found between the dental and basal intercanine depths. This suggested increased variability in the shape of the anterior curvature between the dental and basal arches. Therefore, a future study may be warranted to investigate the variable types of basal arch forms.

The basal intermolar width/depth ratio on CBCT images showed a moderate correlation with its dental counterpart and a weak reverse correlation with dental intermolar depth. This may be explained by the moderate correlation between the dental and basal intermolar depths. Moreover, the dental intercanine width/depth ratio demonstrated a weak reverse correlation with the basal intermolar depth, which might suggest a tendency for a flatter dental archform with smaller basal molar depth.

The use of 3D virtual models has great advantages over plaster models since electronic storage and higher measurement accuracy is assured.<sup>33-35</sup> However, virtual models are time-consuming and costly to generate, and so the application of CBCT offers an attractive alternative for the measurement of arch dimensions as its accuracy and reliability have also been shown.<sup>36-38</sup> Nevertheless, the high radiation dose poses the main disadvantage of the CBCT. A recent study reported that CBCT machines are capable of delivering an effective dose, triple that required for a dental panoramic view.<sup>39</sup> Nevertheless, the benefits of CBCT imaging should be weighed against the radiation dose separately for each case.

Measurements taken from RC and WALA points showed only moderate correlations at the intercanine and intermolar widths (Figure 4 and Table III). This may suggest that there was a consistent thickness of bone and soft tissue labial and buccal to RC points which represented the horizontal distance between the RC and WALA points. However, as these were not strong correlations, considerable variability may exist. While the WALA ridge has been used in previous studies, questions arise regarding its reliability and usefulness in representing the basal arch, as basal bone may not be changed by orthodontic forces, unlike the alveolar bone.<sup>29</sup> Furthermore, the lack of association

between WALA and RC derived depths and ratios may be due to a variation in the location of the RC points which are dependent on the inclination of the roots compared to the fixed position of the WALA points vertically under the FA point.

The present study attempted to find reference points in basal bone so that an accurate evaluation of basal arch could be made. A new landmark (RC) at the level of COR of each tooth was defined on the CBCT scan and the relationship between the arch form measurements from the RC points and those from the WALA points was assessed. It was found that the RC point corresponded to the WALA point and approximated the COR of each tooth. Anatomically, the arch represented by the RC points might not be located in basal bone; however, using a landmark such as the apex of the root to define basal arch form would not be reliable due to the high variability in root position and shape. Therefore, since it is important to preserve arch form during treatment, a constructed landmark such as the RC point may, more accurately, represent clinical basal arch form.

The centre of resistance for anterior teeth was located one third to one half of the root length measured from the alveolar crest. The centre of resistance for posterior teeth was located at 0.3 to 0.4 of the root length.<sup>25,40,41</sup> RC points were digitised on a single transverse section at the level of the coronal third of the canine roots because applying separate transverse sections for the COR for each tooth would not produce consistent basal arch forms. Also, since the average root lengths of mandibular teeth ranged from 12.6 mm to 15.9 mm,<sup>42</sup> the maximum difference in the length of one third of the root between teeth was approximately 1.0 mm which was considered negligible. Therefore, the transverse section at the level of the coronal third of the canine roots was applied for consistent basal arch forms (Figures 1b and 2).

The mandibular arch form was analysed due to its clinical importance in arch wire selection. A previous study demonstrated a strong correlation between the mandibular and maxillary arch forms.<sup>29</sup> Therefore, it was expected that the maxillary arch would be similarly valuable in arch wire selection. In addition, Tai et al.<sup>30</sup> measured the intermolar arch widths through the coronal section of CBCT images to determine arch dimensions. However, the present measurements were performed on an axial cut on the 3D rendered view for easier digitisation of all teeth and accurate recognition

of the centre of the root in the anteroposterior and mediolateral directions.

Further study is needed to determine whether anatomical landmarks other than RC points could serve as a more precise representation of basal bone. In addition, the relationship between the dental and basal arch dimensions using CBCT in other malocclusion groups requires evaluation.

## Conclusions

Only the intercanine and intermolar widths measured on 3D virtual models (WALA points) showed moderate correlation with similar measurements on CBCT (RC points), whereas the canine and molar depths showed no correlation. Hence, the WALA points might not provide an accurately superior representation of basal arch form. RC points could be more identifiable and useful landmarks for basal arch form evaluation.

Dental and basal arch form widths, measured on CBCT images, were strongly correlated in the anterior and posterior segments of normal occlusions. The basal intercanine width showed moderate correlation with dental intermolar width and depth. It is therefore recommended that these relationships are assessed during treatment planning to achieve coordination between the dental and basal arches.

## Corresponding author

Dr Yoon-Ah Kook  
Department of Orthodontics  
Seoul St. Mary's Hospital  
The Catholic University of Korea  
505 Banpo-Dong, Seocho-Gu  
Seoul, 137-701  
Korea

Email: kook190036@yahoo.com

## References

1. Betts NJ, Vanarsdall RL, Barber HD, Higgins-Barber K, Fonseca RJ. Diagnosis and treatment of transverse maxillary deficiency. *Int J Adult Orthodon Orthognath Surg* 1995;10:75-96.
2. Lundström AF. Malocclusion of the teeth regarded as a problem in connection with the apical base. *Int J Orthod Oral Surg Radiogr* 1925;11:1022-42.
3. Proffit WR, Fields HW, Sarver DM. Limitations, controversies, and special problems. In: Proffit WR, Fields HW, Sarver DM, eds. *Contemporary Orthodontics*. St Louis: Mosby Elsevier; 2000:276-9.

4. Strang RHW. The fallacy of denture expansion as a treatment procedure. *Angle Orthod* 1949;19:12-22.
5. Handelman CS. The anterior alveolus: its importance in limiting orthodontic treatment and its influence on the occurrence of iatrogenic sequelae. *Angle Orthod* 1996;66:95-109.
6. Hesby RM, Marshall SD, Dawson DV, Southard KA, Casko JS, Franciscus RG et al. Transverse skeletal and dentoalveolar changes during growth. *Am J Orthod Dentofacial Orthop* 2006;130:721-31.
7. Howes AE. A polygon portrayal of coronal and basal arch dimensions in the horizontal plane. *Am J Orthod* 1954;40:811-31.
8. Sergl HG, Kerr WJ, McColl JH. A method of measuring the apical base. *Eur J Orthod* 1996;18:479-83.
9. Tweed CW. A philosophy of orthodontic treatment. *Am J Orthod Oral Surg* 1945;31:74-103.
10. Bayome M, Sameshima GT, Kim Y, Nojima K, Baek SH, Kook YA. Comparison of arch forms between Egyptian and North American white populations. *Am J Orthod Dentofacial Orthop* 2011;139:e245-52.
11. Kim SC. A study on the configurations of Korean normal dental arches for preformed arch wire. *Korean J Orthod* 1984;14:93-100.
12. Kook YA, Nojima K, Moon HB, McLaughlin RP, Sinclair PM. Comparison of arch forms between Korean and North American white populations. *Am J Orthod Dentofacial Orthop* 2004;126:680-6.
13. Merz ML, Isaacson RJ, Germane N, Rubenstein LK. Tooth diameters and arch perimeters in a black and a white population. *Am J Orthod Dentofacial Orthop* 1991;100:53-8.
14. Nojima K, McLaughlin RP, Isshiki Y, Sinclair PM. A comparative study of Caucasian and Japanese mandibular clinical arch forms. *Angle Orthod* 2001;71:195-200.
15. Nummikoski P, Prihoda T, Langlais RP, McDavid WD, Welander U, Tronje G. Dental and mandibular arch widths in three ethnic groups in Texas: a radiographic study. *Oral Surg Oral Med Oral Pathol* 1988;65:609-17.
16. Yun YK, Kook YA, Kim SH, Mo SS, Cha KS, Kim JG et al. Mandibular clinical arch forms in Koreans with normal occlusions. *Korean J Orthod* 2004;34:481-7.
17. Cordato MA. A simple mathematical study of anterior dental relations: Part I. *Aust Orthod J* 1995;13:249-52.
18. Cordato MA. A mathematical study of anterior dental relations: Part II, Incisor and canine overjet. *Aust Orthod J* 1996;14:143-9.
19. Cordato MA. A simple mathematical study of anterior dental relations. Part III: incisor and canine overbite. *Aust Orthod J* 1998;15:75-84.
20. Ferrario VF, Sforza C, Miani A, Jr, Tartaglia G. Maxillary versus mandibular arch form differences in human permanent dentition assessed by Euclidean-distance matrix analysis. *Arch Oral Biol* 1994;39:135-9.
21. Ferrario VF, Sforza C, Miani A, Jr, Tartaglia G. Mathematical definition of the shape of dental arches in human permanent healthy dentitions. *Eur J Orthod* 1994;16:287-94.
22. Lee YC, Park YC. A study on the dental arch by occlusogram in normal occlusion. *Korean J Orthod* 1987;17:279-87.
23. Kim BI, Bayome M, Kim Y, Baek SH, Han SH, Kim SH et al. Comparison of overjet among 3 arch types in normal occlusion. *Am J Orthod Dentofacial Orthop* 2011;139:e253-60.
24. Kook YA, Bayome M, Park SB, Cha BK, Lee YW, Baek SH. Overjet at the anterior and posterior segments: three-dimensional analysis of arch coordination. *Angle Orthod* 2009;79:495-501.
25. Andrews LF, Andrews WA. The six elements of orofacial harmony. *Andrews J* 2000;1:13-22.
26. Ball RL, Miner RM, Will LA, Arai K. Comparison of dental and apical base arch forms in Class II Division 1 and Class I malocclusions. *Am J Orthod Dentofacial Orthop* 2010;138:41-50.
27. Gupta D, Miner RM, Arai K, Will LA. Comparison of the mandibular dental and basal arch forms in adults and children with Class I and Class II malocclusions. *Am J Orthod Dentofacial Orthop* 2010;138:10 e1-8.
28. Ronay V, Miner RM, Will LA, Arai K. Mandibular arch form: the relationship between dental and basal anatomy. *Am J Orthod Dentofacial Orthop* 2008;134:430-8.
29. Kim KY, Bayome M, Kim KT, Han SH, Kim Y, Kim SH et al. Three-dimensional evaluation of the relationship between dental and basal arch forms in normal occlusion. *Korean J Orthod* 2011;41:288-96.
30. Tai K, Hotokezaka H, Park JH, Tai H, Miyajima K, Choi M et al. Preliminary cone-beam computed tomography study evaluating dental and skeletal changes after treatment with a mandibular Schwarz appliance. *Am J Orthod Dentofacial Orthop* 2010;138:262 e1-11.
31. Andrews LF. The six keys to normal occlusion. *Am J Orthod* 1972;62:296-309.
32. Fujita K, Takada K, QianRong G, Shibata T. Patterning of human dental arch wire blanks using a vector quantization algorithm. *Angle Orthod* 2002;72:285-94.
33. Costalos PA, Sarraf K, Cangialosi TJ, Efstratiadis S. Evaluation of the accuracy of digital model analysis for the American Board of Orthodontics objective grading system for dental casts. *Am J Orthod Dentofacial Orthop* 2005;128:624-9.
34. Quimby ML, Vig KW, Rashid RG, Firestone AR. The accuracy and reliability of measurements made on computer-based digital models. *Angle Orthod* 2004;74:298-303.
35. Zilberman O, Huggare JA, Parikakis KA. Evaluation of the validity of tooth size and arch width measurements using conventional and three-dimensional virtual orthodontic models. *Angle Orthod* 2003;73:301-6.
36. Berco M, Rigali PH, Jr, Miner RM, DeLuca S, Anderson NK, Will LA. Accuracy and reliability of linear cephalometric measurements from cone-beam computed tomography scans of a dry human skull. *Am J Orthod Dentofacial Orthop* 2009;136:17 e1-9.
37. Sherrard JF, Rossouw PE, Benson BW, Carrillo R, Buschang PH. Accuracy and reliability of tooth and root lengths measured on cone-beam computed tomographs. *Am J Orthod Dentofacial Orthop* 2010;137:S100-8.
38. El-Bialy AR, Fayed MS, El-Bialy AM, Mostafa YA. Accuracy and reliability of cone-beam computed tomography measurements: Influence of head orientation. *Am J Orthod Dentofacial Orthop* 2011;140:157-65.
39. Ludlow JB, Ivanovic M. Comparative dosimetry of dental CBCT devices and 64-slice CT for oral and maxillofacial radiology. *Oral Surg Oral Med Oral Pathol Oral Radiol Endod* 2008;106:106-14.
40. Burstone CJ, Pryputniewicz RJ. Holographic determination of centers of rotation produced by orthodontic forces. *Am J Orthod* 1980;77:396-409.
41. Burstone CJ, Pryputniewicz RJ, Weeks R. Centers of resistance of the human mandibular molars. *J Dent Res* 1981;60:515.
42. Scheid RC, Weiss G, Woelfel JB. *Woelfel's Dental Anatomy*. Philadelphia: Wolters Kluwer Health/Lippincott Williams & Wilkins; 2012:41.